

Electrorheological effect and directional non-Newtonian behavior in a nematic capillary subjected to a pressure gradient

Carlos I. Mendoza*

Instituto de Investigaciones en Materiales, Universidad Nacional Autónoma de México, Apdo. Postal 70-360, 04510 México, DF, Mexico

A. Corella-Madueño

Departamento de Física, Universidad de Sonora, Apartado Postal 1626 Hermosillo, Sonora, Mexico

J. Adrián Reyes

Instituto de Física, Universidad Nacional Autónoma de México, Apartado Postal 20-364 01000 México, D. F., Mexico
(Received 12 April 2007; revised manuscript received 5 September 2007; published 30 January 2008)

We consider a capillary consisting of two coaxial cylinders whose core is filled with a nematic liquid crystal (LC) subjected to the simultaneous action of both a pressure gradient applied parallel to the axis of the cylinders and a radial low frequency electric field. We find the configuration of the director of the nematic, initially with an escaped-like configuration, for the flow aligning LC 4'-*n*-pentyl-4-cyanobiphenyl (5CB) by assuming hard anchoring hybrid boundary conditions. Also, we obtain the velocity profile parametrized by the electric field and the pressure gradient for nonslip boundary conditions. Finally, we calculate exactly the effective viscosity, the first normal stress difference, and the dragging forces on the cylinders. The results show an important electrorheological effect and a directional non-Newtonian response with regions of flow thinning and thickening.

DOI: [10.1103/PhysRevE.77.011706](https://doi.org/10.1103/PhysRevE.77.011706)

PACS number(s): 61.30.Gd, 47.57.Lj, 47.65.Gx, 47.27.nf

I. INTRODUCTION

There has been considerable interest in the use of rheological materials to design a large variety of electrorheological (ER) devices. These materials are essentially fluids that contain solid particles in suspension and that react to an applied electric field by showing dramatic and significant changes in their viscosity and other material properties. For instance, an ER fluid undergoes a transition from a liquid state into a viscoelastic solid-like state under the application of a strong electric field [1] that manifests as a large reversible augment in its viscosity. The systems that usually exhibit this ER transition are composed of individual particles that become polarized by the applied field, and align themselves into chains and filaments giving rise to a structure that is responsible for the gelationlike transition mentioned above. This occurs, for example, in concentrated colloidal suspensions of solid particles in a dielectric medium or in some special polymeric fluids [2].

On the other hand, liquid crystals (LC) are fluids that show long-range orientational order over distances many times larger than the dimensions of their molecules [3]. The intrinsic anisotropy of their molecules engenders macroscopic properties that are also anisotropic, as for instance, the dielectric constant and the magnetic susceptibility. These properties may also be modified by the action of external fields. The use of LC as ER fluids put forward obvious advantages over the more conventional ER fluids made of suspended particles. For example, the homogeneity is of par-

ticular importance for microsystems since small channels are easily obstructed by suspended particles [4]. In addition, the homogeneity of LC avoids the problems associated with the settling of the dispersed phase, like agglomeration or sedimentation; these complications are inexistent for LC.

Remarkable non-Newtonian phenomena have been predicted in nematic liquid crystals under shearing conditions [5] and in the vicinity of a nematic isotropic transition [6]. Also, in twisted nematic devices the optical bounce effect has been studied and explained in terms of back flows [7]. The feasibility of liquid crystal systems to produce a practical ER fluid has been demonstrated by Yang *et al.* [8], who have observed an increase of one order of magnitude of the viscosity of a solution of a polymeric liquid crystal when acted upon an external electric field in a rotational rheometer. Recent measurements on a rectangular microchannel filled with a nematic liquid crystal revealed high changes in the flow resistance as a function of an applied electric field [4]. Rodríguez *et al.* [9] have developed a model for studying the ER effect in flowing polymeric nematics. In this model, they proposed an asymptotic formalism to describe a pressure-driven flow in planar cells and found an electrically induced enhanced viscosity. For rectangular cells of polymeric nematics Reyes *et al.* [10] have constructed a hydrodynamic model to analyze the competition between a constant electric field and a uniform shear flow.

However, in spite of the ample amount of ER devices that have been developed [1], our understanding of the basic mechanisms responsible for the ER effect is, in general, poor. The aim of this work is to study the response of a nematic liquid crystal confined to the region between two coaxial cylinders and subjected to the action of a constant pressure drop along the axis of the cylinder and a radial low fre-

*Author to whom correspondence should be addressed. FAX: +52(55)56161201, cmendoza@iim.unam.mx

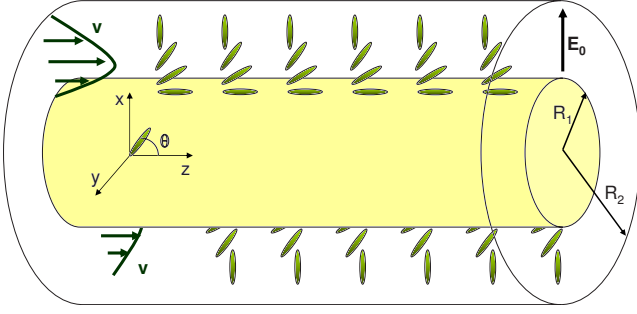


FIG. 1. (Color online) Schematics of a nematic liquid crystal confined by two coaxial cylinders and subjected to a radial electric field and a pressure gradient.

quency electric field generated by a potential difference imposed between both cylinders.

The outline of the paper is as follows: In Sec. II we write the nematodynamic equations for our system. Then, we consider the particular case of a pressure-driven flow (Poiseuille) and derive equations for the stationary orientational and velocity profiles. In Sec. III, we use these equations to calculate the apparent viscosity and, in Sec. IV, we calculate the first normal stress difference, N_1 , as a function of the applied electric field, and the external imposed pressure. Finally, in Sec. V, we discuss our results and present the conclusions.

II. NEMATIC CONFIGURATION AND VELOCITY PROFILE

Consider a pure thermotropic nematic confined between two coaxial pipes with radii R_1 and R_2 , under the action of a radial low frequency electric field, as depicted in Fig. 1. Under these conditions, the director's configuration is spatially homogeneous along the axis of the pipe and varies with r so that, in a cylindrical coordinate system, the director varies as

$$\hat{\mathbf{n}} = [\sin \theta(r), 0, \cos \theta(r)], \quad (1)$$

and we assume that it satisfies the hybrid hard anchoring conditions

$$\theta(r=R_1) = 0, \quad \theta(r=R_2) = \pi/2, \quad (2)$$

where $\theta(r)$ is the orientational angle defined with respect to the z axis, as shown in Fig. 1. We also assume that the nematic is subjected to a constant pressure drop along the axis of the cylinder that produces a shear flow profile along the region confined by both cylinders given by

$$\mathbf{v} = [0, 0, v_z(r)], \quad (3)$$

which satisfies the nonslip boundary conditions

$$v_z(r=R_1) = 0, \quad v_z(r=R_2) = 0. \quad (4)$$

Both, hard-anchoring and nonslip boundary conditions restrict the validity of our description to moderate values of the external agents acting against the elastic forces at the cylinder's wall. Nevertheless, use these assumptions since previous calculations [11] done for the apparent viscosity of a nematic in Poiseuille flow using the same assumptions were

in good agreement with experimental data [12]. Therefore, the hard-anchoring and nonslip boundary conditions assumed in our model are correct for flow rates as large as those we shall use here. These moderate pressure gradients guarantee a laminar-flow regime. Larger pressure values may induce oscillating boundary layers and long rolling states for which the director moves out of the shear plane. Even more, in this case, it would be possible to irreversibly switch between topologically distinct states [13].

Using the formulation given in Refs. [14,15], the full nematodynamics which couples the equations of motion for $\hat{\mathbf{n}}$ and the hydrodynamic velocity field \mathbf{v} may be written in the form

$$\begin{aligned} \frac{dn_i}{dt} = & \frac{1}{2}(\partial_k v_i - \partial_i v_k)n_k + \frac{\lambda}{2}(\delta_{il} - n_i n_l)n_k(\partial_k v_l + \partial_l v_k) \\ & + \frac{1}{\gamma_1}(\delta_{im} - n_i n_m)\frac{\delta \mathcal{F}}{\delta n_m} \end{aligned} \quad (5)$$

and

$$\rho \frac{dv_i}{dt} = -\frac{\partial p}{\partial x_i} + \frac{\partial}{\partial x_j}[\sigma_{ij}^r + \sigma_{ij}^d], \quad (6)$$

where ρ and p stand for the mass density and pressure field of the nematic. Here the stress tensor of the nematic $\sigma = \sigma^r + \sigma^d$ has been separated in two contributions: One reactive σ_{ij}^r and the other dissipative σ_{ij}^d . Their explicit expressions are given by

$$\begin{aligned} \sigma_{ij}^r \equiv & -\frac{1}{2}\lambda(n_i h_j + n_j h_i) - \frac{1}{2}\left(\Pi_{jl}\frac{\partial}{\partial x_i}n_l + \Pi_{il}\frac{\partial}{\partial x_j}n_l\right) \\ & - \frac{1}{2}\frac{\partial}{\partial x_l}[(\Pi_{ij} + \Pi_{ji})n_l - \Pi_{il}n_j - \Pi_{jl}n_i], \end{aligned} \quad (7)$$

$$\begin{aligned} \sigma_{ij}^d \equiv & \alpha_1 n_i n_j n_\mu n_\rho v_{\mu\rho} + \alpha_4 v_{ij} \\ & + \frac{(\alpha_3 \alpha_5 - \alpha_2 \alpha_6)}{\gamma_1}(n_i n_\mu v_{\mu j} + n_j n_\mu v_{\mu i}). \end{aligned} \quad (8)$$

Here, the kinetic coefficients α_1 , α_2 , α_3 , α_4 , α_5 , and α_6 are the Leslie coefficients, $\gamma_1 = \alpha_3 - \alpha_2$ is the orientational viscosity, and $\lambda \equiv -\gamma_2/\gamma_1$ is a dimensionless reactive coefficient, with $\gamma_2 = \alpha_2 + \alpha_3$. Due to the Parodi relation [16] $\alpha_2 + \alpha_3 = \alpha_6 - \alpha_5$ only five of these coefficients are independent. In these equations d/dt denotes the material derivative operator and $\partial_k \equiv \partial/\partial x_k$; δ_{il} is the usual Kronecker delta and \mathcal{F} is the total free energy of the nematic, which has an elastic and an electromagnetic contribution. For the present model the elastic part of the free energy is given by

$$\begin{aligned} \mathcal{F}_{el} = & \frac{1}{2} \int_V [K_1(\nabla \cdot \hat{\mathbf{n}})^2 + K_2(\hat{\mathbf{n}} \cdot \nabla \times \hat{\mathbf{n}})^2 \\ & + K_3(\hat{\mathbf{n}} \times \nabla \times \hat{\mathbf{n}})^2] dV, \end{aligned} \quad (9)$$

where the elastic moduli K_1 , K_2 , and K_3 describe transverse bending (splay), torsion (twist), and longitudinal bending (bend) deformations, respectively, and the integration is over

the volume confined by the cylinders. The so-called molecular field h_i is given by

$$h_i \equiv \frac{1}{\gamma_1} (\delta_{im} - n_i n_m) \frac{\delta \mathcal{F}}{\delta n_m}, \quad (10)$$

where the functional derivative $\delta \mathcal{F} / \delta n_m$ reduces to

$$\begin{aligned} \frac{1}{K_1 R_2^2} \frac{\delta \mathcal{F}}{\delta \theta} &= \frac{d^2 \theta}{dx^2} (\cos^2 \theta + \kappa \sin^2 \theta) + \left(\frac{d\theta}{dx} \right)^2 \frac{1}{2} (\kappa - 1) \sin 2\theta \\ &+ \frac{q-1}{2x^2} \sin 2\theta + \frac{1}{x} \frac{d\theta}{dx} (\cos^2 \theta + \kappa \sin^2 \theta), \end{aligned} \quad (11)$$

where $\kappa \equiv K_3 / K_1$ and the tensor Π_{jl} is given by

$$\Pi_{jl} \equiv \partial \mathcal{F} / \partial \left(\frac{\partial}{\partial x_j} n_l \right) - n_r n_l \partial \mathcal{F} / \partial \left(\frac{\partial}{\partial x_j} n_r \right).$$

As usual, the symmetric part of the velocity gradient tensor is

$$v_{jl} \equiv \frac{1}{2} \left(\frac{\partial}{\partial x_j} v_l + \frac{\partial}{\partial x_l} v_j \right). \quad (12)$$

We notice that Eq. (11) does not involve K_2 but only K_1 and K_3 . In other words, the fact that \hat{n} only depends on the variables contained on its own plane causes the absence of twist deformation, so only splay and bend distortions are present.

The electromagnetic part of the free energy, \mathcal{F}_{em} , taking the field \mathbf{E}_0 along the radial direction r is, in MKS units

$$\mathcal{F}_{em} = -\frac{1}{2} \int_V \mathbf{D} \cdot \mathbf{E}_0 dV = -\frac{1}{2} \int_V \epsilon_{rr}(r) E_0^2 dV, \quad (13)$$

where $\epsilon_{rr}(r)$ is an element of the dielectric tensor ϵ_{ij} . Since the nematic is a uniaxial medium, the dielectric tensor can be written as

$$\epsilon_{ij} = \epsilon_{\perp} \delta_{ij} + \epsilon_a n_i n_j, \quad (14)$$

with $\epsilon_a = \epsilon_{\parallel} - \epsilon_{\perp}$ the dielectric anisotropy, and ϵ_{\parallel} and ϵ_{\perp} the parallel and perpendicular dielectric constants of the LC, respectively.

We want to remark that even though Eq. (8) states formally a constitutive relation where the stress tensor seems to be proportional to gradient components of the velocity, the fluid is not Newtonian because the director components n_i are coupled with the velocity field components by means of Eq. (5). Thus, σ is not only an anisotropic relation of the velocity, but is indeed a nonlinear function of the gradient velocity components as we shall see explicitly below.

Using Eqs. (9), (13), and (14), the total free energy, \mathcal{F} , becomes

$$\begin{aligned} \mathcal{F} &= \mathcal{F}_{el} + \mathcal{F}_{em} \\ &= \frac{1}{2} \int_V [K_1 (\nabla \cdot \hat{n})^2 + K_2 (\hat{n} \cdot \nabla \times \hat{n})^2 + K_3 (\hat{n} \times \nabla \times \hat{n})^2] dV \\ &\quad - \pi K_1 R_2 q \int_{R_1}^{R_2} (\sin^2 \theta + \epsilon_{\perp}^s / \epsilon_a^s) \frac{dr}{r}, \end{aligned} \quad (15)$$

where we have employed the electrostatic field \mathbf{E}_0 with

$\equiv -\mathbf{e}_r \Delta \phi / [r \ln(R_2/R_1)]$ generated between two coaxial cylinders subject to a potential difference $\Delta \phi$.

The elastic free energy of the LC is obtained by integrating Eq. (9) over the cylindrical volume. Then, expressing $\nabla \cdot \hat{n}$ and $\nabla \times \hat{n}$ in cylindrical coordinates we obtain the free energy per unit length, $f \equiv \mathcal{F}/L$, with L the length of the cylinders:

$$\begin{aligned} f &= \pi K_1 R_2 \left\{ \int_{R_1/R_2}^1 \left[\left(\frac{d\theta}{dx} \right)^2 (\cos^2 \theta + \kappa \sin^2 \theta) + \frac{\sin^2 \theta}{x^2} \right] x dx \right. \\ &\quad \left. - q \int_{R_1/R_2}^1 (\sin^2 \theta + \epsilon_{\perp}^s / \epsilon_a^s) \frac{dx}{x} \right\}, \end{aligned} \quad (16)$$

where $x = r/R_2$, and q is an important parameter defined as

$$q \equiv \epsilon_a^s \Delta \phi^2 / [K_1 \ln^2(R_2/R_1)], \quad (17)$$

where ϵ_a^s is the low frequency dielectric anisotropy. The parameter q represents the ratio of the electric and elastic energies; for $q \ll 1$ the influence of the applied field is weak, while for $q \gg 1$ the field essentially overcomes the Frank's elastic forces. We should mention that there is no Fredericks transition in this system since we are using the hybrid boundary conditions given by Eq. (2).

Therefore, Eqs. (5) and (6) can be written as

$$\begin{aligned} 0 &= \frac{d^2 \theta}{dx^2} (\cos^2 \theta + \kappa \sin^2 \theta) + \left(\frac{d\theta}{dx} \right)^2 \frac{1}{2} (\kappa - 1) \sin 2\theta \\ &+ \frac{q-1}{2x^2} \sin 2\theta + \frac{1}{x} \frac{d\theta}{dx} (\cos^2 \theta + \kappa \sin^2 \theta) \\ &+ \left(-\frac{dp}{d\zeta} \frac{x}{2} + \frac{b}{R_2 x} \right) \frac{R_2^2}{K_1 g(\theta)} (\cos 2\theta - \cos 2\theta_0), \end{aligned} \quad (18)$$

$$\frac{dv_z}{dx} = \frac{2R_2}{\gamma_2 g(\theta)} \left[-\frac{dp}{d\zeta} \frac{x}{2} + \frac{b}{R_2 x} \right], \quad (19)$$

where b is an integration constant and $\zeta \equiv z/R_2$. After decoupling both equations [11], we obtain the following equation for $\theta(x)$:

$$\begin{aligned} 0 &= \frac{d^2 \theta}{dx^2} x^2 (\cos^2 \theta + \kappa \sin^2 \theta) + \left(\frac{d\theta}{dx} \right)^2 \frac{x^2}{2} (\kappa - 1) \sin 2\theta \\ &+ \frac{q-1}{2} \sin 2\theta + x \frac{d\theta}{dx} (\cos^2 \theta + \kappa \sin^2 \theta) \\ &- \frac{\Lambda}{g(\theta)} x^2 \left[x + \frac{b'}{x} \right] (\cos 2\theta - \cos 2\theta_0), \end{aligned} \quad (20)$$

where $b' = -bR_2 / (K_1 \Lambda)$ while for v_z we obtain

$$v_z(x) = v_0 \Lambda \left[\int_x^1 \frac{s}{g(\theta(s))} ds + b'' \int_x^1 \frac{ds}{s g(\theta(s))} \right], \quad (21)$$

$$b'' \equiv - \frac{\int_{R_1/R_2}^1 \frac{s}{g(\theta(s))} ds}{\int_{R_1/R_2}^1 \frac{ds}{sg(\theta(s))}}, \quad (22)$$

and $v_0 \equiv 2K_1/R_2$. Here, we have applied the boundary conditions given by Eqs. (4) to obtain the velocity profile Eq. (21). In these equations $\cos 2\theta_0 = -\gamma_1/\gamma_2$ and

$$g(\theta) = [2\alpha_1 \sin^2 \theta \cos^2 \theta + (\alpha_5 - \alpha_2) \sin^2 \theta + (\alpha_6 + \alpha_3) \cos^2 \theta + \alpha_4]. \quad (23)$$

Notice that in Eq. (21) $g(\theta)$ plays the role of a position dependent viscosity [17] which is larger at the pipe border than at the inner cylinder due to the boundary conditions.

In the previous equations, Λ is a dimensionless parameter defined as

$$\Lambda \equiv \frac{1}{2} \frac{dp}{d\zeta} \frac{R_2^2}{K_1}, \quad (24)$$

and represents the ratio of the hydrodynamic and elastic energies; for $\Lambda \ll 1$ the influence of the applied pressure gradient is weak, while for $\Lambda \gg 1$ the flow essentially overcomes the elastic energy. Note that the influence of the pressure gradient is greatly augmented for a large pipe radius R_2 .

Once $\theta(x)$ has been determined numerically from Eqs. (20) and (2) it can be inserted into Eq. (21) to obtain numerically $v_z(x)$.

In what follows, we will present results for the specific case of 4'-n-pentyl-4-cyanobiphenyl (5CB) liquid crystal. The parameters used were $T_{IN}-T=10$ °C with $T_{IN}=35$ °C, $\kappa=1.316$, $K_1=1.2 \times 10^{-11}$ N, $\alpha_1=-0.0060$ Pa s, $\alpha_2=-0.0812$ Pa s, $\alpha_3=-0.0036$ Pa s, $\alpha_4=0.0652$ Pa s, $\alpha_5=0.0640$ Pa s, $\alpha_6=-0.0208$ Pa s, $\gamma_1=0.0777$ Pa s, $\gamma_2=-0.0848$ Pa s [18], and $R_1/R_2=0.5$.

It is convenient to remark that the working temperature is not near enough from the transition temperature to expect critical fluctuations. However, thermal fluctuations in \hat{n} are present and observable by the scattering of optical fields. This effect is considerably reduced by the presence of the imposed low frequency electric field which is used to decrease the correlation length in \hat{n} [3].

In Fig. 2 we plot the configuration θ as a function of x parametrized by q and Λ . Notice first the presence of the undistorted state corresponding to $\Lambda=0$ and $q=0$ which is similar to the well known escaped configuration. As can be seen for $q=50$, \hat{n} is much more aligned with the radial direction than for $q=0$. This is expected because the director tends to be aligned in the direction of the electric field. For positive $\Lambda > 0$, corresponding to negative velocity, \hat{n} tends to be aligned in the axial direction whereas for negative $\Lambda < 0$ the trend is the opposite. Nevertheless, for $q=50$ the influence of the pressure gradient is shadowed by the action of the electric field, especially at regions near the inner cylinder. In the cases, $\Lambda=-50$ and $\Lambda=0$, the sign of the concavity of the curves is the same but it is more pronounced for the case $\Lambda=-50$, for which θ may overpass the boundary value $\theta=90^\circ$ by a small amount in a region near the external cylinder.

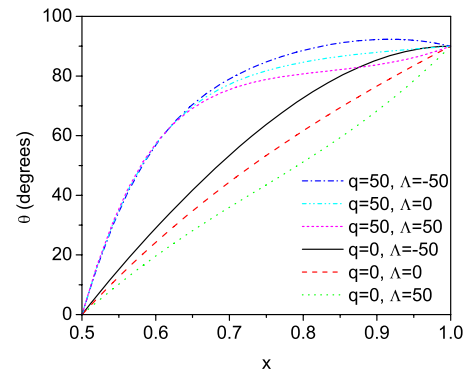


FIG. 2. (Color online) Nematic's configuration θ as a function of x for 5CB and $R_1/R_2=0.5$.

der. In contrast, in the case $\Lambda=+50$ the curves exhibit concavity changes.

In Fig. 3 we show the typical velocity profile v_z for different values of Λ and an arbitrary value of the electric field (in the figure $q=50$). As it is expected, the magnitude of the velocity increases, at every point in the pipe, for increasing values of the magnitude of the parameter Λ . Also, Fig. 3 exhibits a clear difference in the magnitude of the velocity between forward and backward flows, which is a consequence of the asymmetry of the undistorted director's configuration (escaped configuration). Moreover, the position of the extrema of the curves, given by $dv_z/dx=0$, and which represent a vanishing shear stress, are closer to the inner cylinder in all the curves, with no significant dependence on the value of Λ . This is in contrast to the case of a Newtonian flow for which the maxima is approximately at the middle of the distance between both cylinders [19]. In Fig. 4 we plot the velocity profile v_z for different values of q and two arbitrary values of the pressure gradient [(a) $\Lambda=50$ and (b) $\Lambda=-50$]. This figure shows that the application of the electric field affects the velocity of the fluid mainly in the central part of the pipe while the velocity near the walls remains practically unaltered. We also observe a shift of the extrema of the velocity curves towards the center of the pipe and a reduction of the asymmetry with respect to the direction of the flow for increasing values of the electric field, indicating a tendency to adopt a Newtonian behavior. Moreover, the

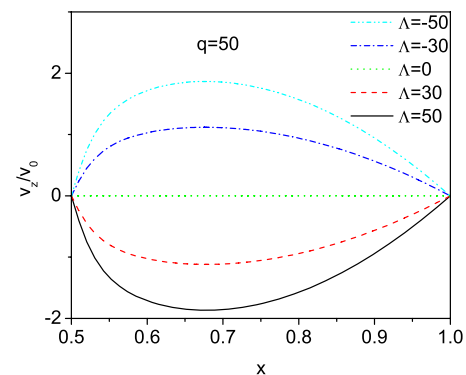


FIG. 3. (Color online) Velocity profiles v_z vs x for 5CB. The parameters used were $R_1/R_2=0.5$ and $q=50$.

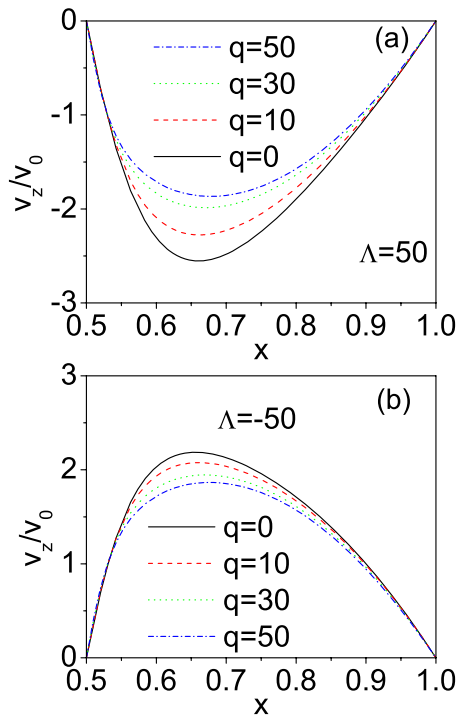


FIG. 4. (Color online) Velocity profiles v_z vs x for 5CB. The parameters used were $R_1/R_2=0.5$, (a) $\Lambda=50$, and (b) $\Lambda=-50$.

velocity profile is more affected by the electric field in the case of backward flow than in the case of forward flow. This asymmetry is a consequence of the fact that the undistorted configuration is disposed in such a way that its director goes from $\theta=0$ at the inner cylinder to $\theta=\pi/2$ at the outer cylinder in a counterclockwise way. If director's configuration were the opposite, that is, if it went from $\theta=0$ at the inner cylinder to $\theta=\pi/2$ at the outer cylinder in a clockwise way, then the response to the external flow would be also opposite. Therefore, this could be a way to determine in which sense the escaped configuration is actually placed. In general, it can be asserted that the displacement of the extrema in the velocity profiles is caused by the configuration distortions induced by the coupling between the pressure-driven velocity and the electrically aligned nematic director.

III. BIASED ELECTRORHEOLOGICAL EFFECT

The viscosity function or apparent viscosity, η , is the quotient between the shear stress and the magnitude of the local

strain rate. It is a function of the nematic's director by means of the expression Eq. (23) [17,20,21]. Since the orientational angle θ is strongly dependent on the electric field and since η depends on θ , it follows that the behavior of the system is non-Newtonian.

From Eqs. (20) and (23) we obtain the spatial variation of $g(\theta)$ within the pipe. To define a global property of the whole capillary, we integrate the result over the cross section of the pipe to obtain the averaged apparent viscosity

$$\bar{\eta}(q, \Lambda) \equiv \frac{R_2^2}{R_2^2 - R_1^2} \int_{R_1/R_2}^1 g(\theta(x); q, \Lambda) x dx.$$

If we now plot $\bar{\eta}(q, \Lambda)$ as a function of q and Λ , we get the results displayed in Fig. 5. Panel (a) shows that $\bar{\eta}$ always increases as a function of the electric field q for any given pressure gradient Λ . Furthermore, for the largest value of q considered ($q=50$), the value of $\bar{\eta}$ for the largest backward flow ($\Lambda=50$) increases about 50% with respect to its value in the absence of electric field, whereas it increases only about 20% for the largest forward flow ($\Lambda=-50$). In this sense we can say that electrorheological effects are more evident for backward flow than for forward flow. The reason why the viscosity increases with increasing electric field is that the nematic's director is more aligned with the direction of the field that is perpendicular to the direction of flow. On the other hand, in Fig. 5(b), we observe that for a given value of the electric field and for the range of flow considered ($-50 < \Lambda < 50$) the viscosity decreases as Λ increases. This means that for backward flow ($\Lambda > 0$) the viscosity decreases as the magnitude of the flow increases whereas for forward flow ($\Lambda < 0$) the viscosity increases as the magnitude of the flow increases. Therefore, we have flow thinning in one direction and flow thickening in the other. This directional response is due to the fact that the initial undistorted nematic configuration is asymmetrical. Therefore, for backward flow this configuration is distorted so that nematic's molecules are more paralleled oriented in the direction of the flow decreasing the viscosity while in the forward flow the nematic's molecules adopt a more perpendicular position with respect to the direction of the flow increasing the viscosity. Also, in the forward case most of the mechanical energy is elastically accumulated in deforming the nematic's configuration instead of being used to move the fluid, as compared to the backward case. In this sense the undistorted configuration is playing the role of a biased spring inherent to the liquid, which is stiffer in one direction than in the other.

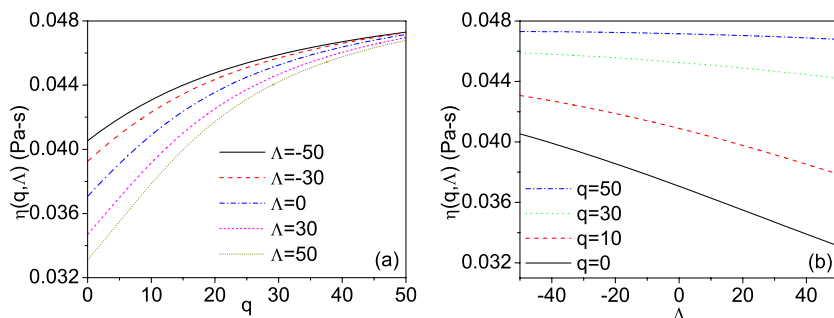


FIG. 5. (Color online) Averaged apparent viscosity as a function of (a) the electric field q and (b) the pressure gradient Λ .

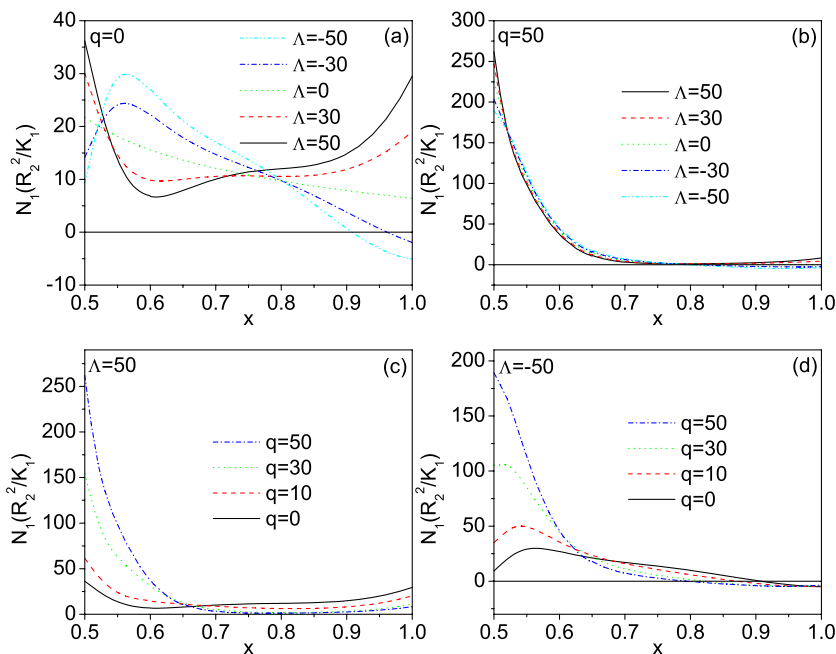


FIG. 6. (Color online) First normal stress difference N_1 vs x . (a) $q=0$, (b) $q=50$, (c) $\Lambda=50$, and (d) $\Lambda=-50$.

IV. FIRST NORMAL STRESS DIFFERENCE

Under conditions of shear flow, non-Newtonian fluids usually show positive steady-state first normal stress difference, N_1 , over a range of shear rates. Also, N_1 is zero or positive for isotropic fluids at stationary flows over all shear rates. In liquid crystalline solutions, positive normal stress differences are found at low and high shear rates, while negative values occur at intermediate shear rates [20].

On the other hand, Marrucci *et al.* [22] have solved a two dimensional version of the Doi model for nematics [23] in which the molecules are assumed to lie in the plane perpendicular to the vorticity axis, that is, in the plane parallel to both, the direction of the velocity and the direction of the velocity gradient. Despite this simplification, for strong enough shear rates over which N_1 is negative, Doi model is in excellent agreement with observations. This result suggests the possibility that negative first normal stress differences may be produced in a two-dimensional flow. Nevertheless, this is not the case for the Leslie-Ericksen approach adopted in this paper as we shall see.

Let us now examine the effects produced by the stresses generated after the reorientation process has taken place by calculating the viscometric functions which relate the shear and normal stress differences. For the geometry under consideration and using the convention of Ref. [24], the first normal stress difference is defined by

$$N_1 \equiv \sigma_{zz} - \sigma_{rr}. \quad (25)$$

Inserting Eqs. (5) and (3) into Eqs. (8), (7), and (25) we get

$$N_1 = \frac{K_1}{R_2^2} \left(\frac{d\theta}{dx} \right)^2 (\cos^2 \theta + \kappa \sin^2 \theta) + \frac{1}{2R_2} \frac{dv_z(x)}{dx} \{ [\alpha_1(\sin \theta - \cos \theta) + \alpha_5 + \alpha_6] \cos 2\theta - \lambda(\alpha_2 + \alpha_3) [\sin \theta + \cos \theta + \cos 2\theta - \cos 2\theta_0] \sin 2\theta \}, \quad (26)$$

which has been expressed in terms of the already calculated quantities $v_z(x)$ and $\theta(x)$.

Various plots of N_1 versus x for 5CB and several values of q and Λ are displayed in Fig. 6 which shows the asymmetry between the backward and forward responses due to the pressure gradient. A direct comparison between Figs. 6(a) and 6(b) shows that this asymmetry is strongly diminished by the presence of the electric field that gets together in Fig. 6(b) those curves which are widely separated in Fig. 6(a) for different values of Λ .

Figures 6(c) and 6(d) show N_1 parametrized by q for $\Lambda=50$ and $\Lambda=-50$, respectively. The plot confirms that the effect of the field over N_1 is to diminish the biased response to the sign of the pressure gradient. This means that the directional response and non-Newtonian behavior of the nematic is smaller for stronger fields because this restrains greatly the response to the pressure drop.

The integration of the first normal stress difference profile over the cross section of the pipe,

$$\overline{N_1}(q, \Lambda) = \frac{2R_2^2}{R_2^2 - R_1^2} \int_{R_1/R_2}^1 N_1(\theta(x); q, \Lambda) x dx,$$

renders the averaged first normal stress difference. This is shown in Figs. 7(a) and 7(b) where we have plotted $\overline{N_1}$ as a function of q and Λ . As can be seen from Fig. 7(a), $\overline{N_1}$ depends almost linearly on q for backward flow, $\Lambda=-50$, whereas it exhibits a minimum at $q=10$ for forward flow $\Lambda=50$. Figure 7(b) displays clearly how contrasting is the difference between forward and backward flows for small values of the electric field q where a local minimum moves to the right as Λ increases. Also, it is clear that the degree of the directional dependent non-Newtonian behavior of this confined nematic can be electrically controlled. We should mention that even though there is a small region near the outer cylinder for which N_1 has small negative values,

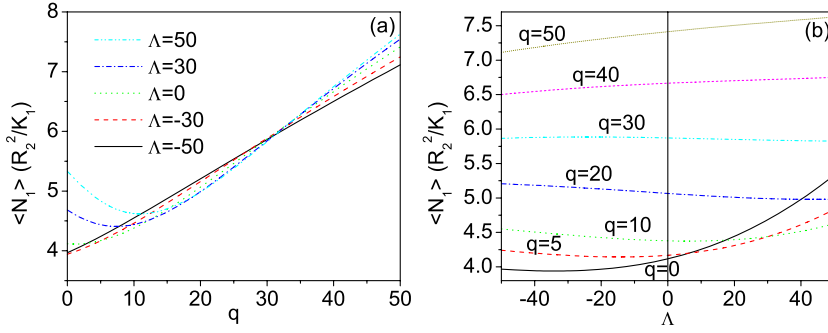


FIG. 7. (Color online) Averaged first normal stress difference as a function of (a) q and (b) Λ .

$\overline{N_1}(q, \Lambda)$ which is a quantity providing the global behavior, is always positive because those regions represent only a small portion of the whole section of the liquid crystal.

It is also useful to calculate the only nonvanishing stress component σ_{rz} from Eq. (8). We find, after doing similar manipulations to those used to obtain Eq. (26), that

$$\begin{aligned} \sigma_{rz} = & \frac{1}{2R_2} (\alpha_1 \sin^2 \theta \cos^2 \theta + \alpha_4 + \alpha_5 \sin^2 \theta \\ & + \alpha_6 \cos^2 \theta) \frac{dv_z(x)}{dx} + \frac{1}{2} (\alpha_2 - \alpha_3) \sin 2\theta \left[\frac{\lambda}{2} (\sin \theta \right. \\ & \left. + \cos \theta) \frac{dv_z(x)}{dx} + \frac{\Lambda}{g(\theta)} \left[x + \frac{b'}{x} \right] (\cos 2\theta - \cos 2\theta_0) \right], \end{aligned}$$

which evaluated on both cylindrical walls and integrated over the surface of each cylinder, provides the dragging forces, D_1 and D_2 , per unit of cylinder length, exerted on each cylinder by the flowing nematic. The explicit expressions of these forces can be written, respectively, as

$$D_1 = 2\pi R_1 \sigma_{rz} \Big|_{x=R_1/R_2} \quad (27)$$

$$= \frac{\pi R_1}{R_2} (\alpha_4 + \alpha_6) \frac{dv_z(x)}{dx} \Big|_{x=R_1/R_2} \quad (28)$$

$$= \frac{\pi R_1 (\alpha_4 + \alpha_6) v_0 \Lambda \gamma_2}{R_2 (\alpha_3 + \alpha_4 + \alpha_6)} \left[\frac{R_1}{R_2} + \frac{R_2 b''}{R_1} \right], \quad (29)$$

$$D_2 = 2\pi R_2 \sigma_{rz} \Big|_{x=1} \quad (30)$$

$$= \pi (\alpha_4 + \alpha_5) \frac{dv_z(x)}{dx} \Big|_{x=1} \quad (31)$$

$$= - \frac{\pi (\alpha_4 + \alpha_5) v_0 \Lambda \gamma_2}{(\alpha_4 - \alpha_2 + \alpha_5)} (1 + b''). \quad (32)$$

In Fig. 8, we plot D_1 and D_2 as a function of q and Λ . We observe that both D_1 and D_2 have an almost constant value as a function of q , but a linear decrease as a function of Λ .

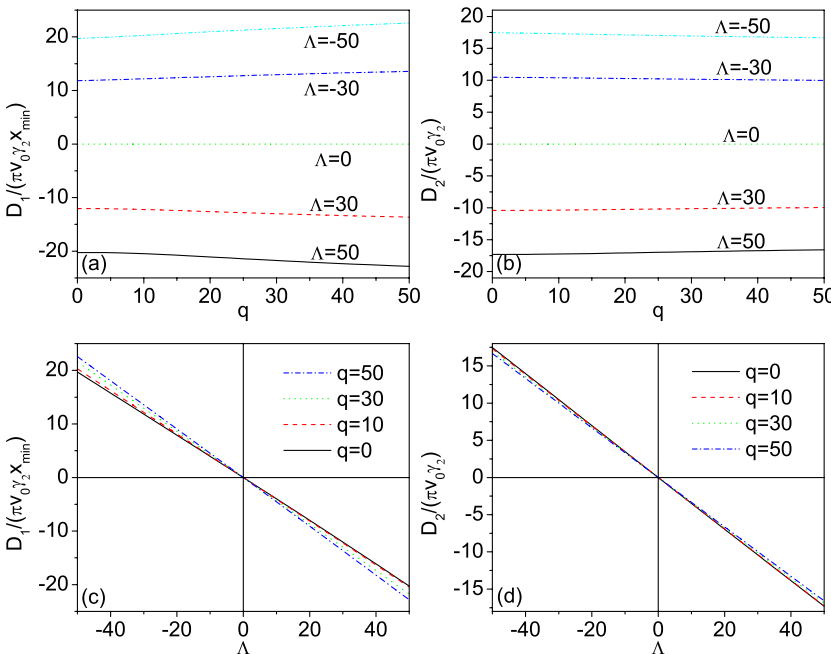


FIG. 8. (Color online) Dragging forces, D_1 and D_2 , at the surfaces of the capillary as a function of q and Λ .

V. CONCLUDING REMARKS

We have constructed a hydrodynamic model for a nematic liquid crystal that is confined between two coaxial cylinders and subjected to the simultaneous action of a radial electric field and an external pressure gradient. Using the Ericksen-Leslie-Parodi nematodynamics, we have written and solved numerically the exact stationary equations for the director's configuration and velocity profile. The non-Newtonian effects are clearly manifested in the behavior of the velocity profiles whose maximum or minimum move toward the inner pipe with respect to the corresponding Newtonian case. Moreover, the effect of the electric field is present mainly in the central part of the capillary whilst the action of the pressure gradient affects the velocity at all the points of the pipe, including the regions near the walls.

We have shown that the reorientation produced by the electric field gives rise to an augment in the apparent average viscosity of the LC as a function of the applied electric field (electrorheological effect). The viscosity is also dependent on the value of the pressure gradient giving rise to a non-Newtonian behavior. Even more, the viscosity depends not only on the magnitude of the pressure gradient but also on the direction of the flow with flow thinning in one direction and flow thickening in the other.

Also, we have found that the spatial distribution of the first normal stress difference is positive in all the cross section of the pipe except near the outer cylinder where a small

negative region is present. From this quantity, we have derived the averaged first normal stress difference and found that it is positive for all values of the pressure gradient and electric field.

Finally, we have calculated the dragging forces on the inner and outer cylinders and found an almost constant value for different electric fields and a monotonic decrease as a function of the pressure gradient.

It is important to point out that these directional and non-Newtonian behavior of the confined liquid crystal are a consequence of the coupling between the velocity field and the escaped-like undistorted configuration. For this reason, the nematic is able to store more elastic energy in one direction than in the other.

We expect that our results on the non-Newtonian dynamics of the nematic in a capillary and their electrorheological manifestations could stimulate further theoretical and experimental studies. In particular, the fact that this system shows a directional response that can be electrically modified makes it ideally suited for the design of various electrically controlled devices with asymmetric non-Newtonian behavior.

ACKNOWLEDGMENTS

We acknowledge the partial support of the Programa Interinstitucional de Colaboración UNISON-UNAM, and the DGAPA-PAPIIT Grants Nos. IN-117606 and IN-107607.

-
- [1] *Electrorheological Fluids*, edited by L. R. Tao (World Science Publishers, New York, 1992).
- [2] H. Block and J. P. Kelly, *J. Phys. D* **21**, 1661 (1988).
- [3] P. G. de Gennes, *The Physics of Liquid Crystals* (Clarendon, Oxford, 1964).
- [4] M. De Volder, K. Yoshida, S. Yokota, and D. Reynaerts, *J. Micromech. Microeng.* **16**, 612 (2006).
- [5] A. D. Guillén and C. I. Mendoza, *J. Chem. Phys.* **126**, 204905 (2007); A. D. Guillén and C. I. Mendoza, *J. Chem. Phys.* **127**, 059901 (2007).
- [6] C. Y. David Lu, P. D. Olmsted, and R. C. Ball, *Phys. Rev. Lett.* **84**, 642 (2000); X. F. Yuan and L. Jupp., *Europhys. Lett.* **60**, 691 (2002); D. Marenduzzo, E. Orlandini, and J. M. Yeomans, *Europhys. Lett.* **64**, 406 (2003).
- [7] N. J. Smith, M. D. Tillin, and J. R. Sambles, *Phys. Rev. Lett.* **88**, 088301 (2002).
- [8] I. K. Yang and A. D. Shine, *J. Rheol.* **36**, 1079 (1992).
- [9] R. F. Rodríguez, J. A. Reyes, and O. Manero, *J. Chem. Phys.* **110**, 8197 (1999).
- [10] J. A. Reyes, O. Manero, and R. F. Rodríguez, *Rheol. Acta* **40**, 426 (2001).
- [11] R. J. Atkin, *Arch. Ration. Mech. Anal.* **38**, 224 (1970); H. C. Tseng, D. K. Siver, and B. A. Finlayson, *Phys. Fluids* **15**, 1213 (1972).
- [12] J. Fisher and A. G. Frederickson, *Mol. Cryst. Liq. Cryst.* **6**, 255 (1969).
- [13] C. Denniston, E. Orlandini, and J. M. Yeomans, *Comput. Theor. Polym. Sci.* **11**, 389 (2001).
- [14] L. D. Landau and E. M. Lifshitz, *Theory of Elasticity* (Pergamon, Oxford, 1986).
- [15] M. Kleman and O. D. Lavrentovich, *Soft Matter Physics: An Introduction* (Springer-Verlag, New York, 2003).
- [16] O. Parodi, *J. Phys. (Paris)* **31**, 581 (1970).
- [17] T. Carlsson, *Mol. Cryst. Liq. Cryst.* **104**, 307 (1984).
- [18] Ian W. Stewart, *The Static and Dynamic Continuum Theory of Liquid Crystals* (Taylor & Francis, London, 2004).
- [19] L. D. Landau and Lifshitz, *Fluid Mechanics*, 2nd ed. (Pergamon, Oxford, 2003).
- [20] G. Kiss and R. S. Porter, *J. Polym. Sci., Polym. Symp.* **65**, 193 (1978).
- [21] M. Miesowicz, *Nature (London)* **17**, 261 (1935).
- [22] G. Marrucci and P. L. Maffettone, *Macromolecules* **22**, 4076 (1989).
- [23] M. Doi and S. F. Edwards, *The Theory of Polymer Dynamics* (Oxford University Press, New York, 1986).
- [24] R. B. Bird, R. C. Armstrong, and O. Hassager, *Dynamic of Polymeric Liquids*, Vol. 1 (Wiley, New York, 1977).